Turkish Journal of Physics

http://journals.tubitak.gov.tr/physics/

Invited Review Article

Turk J Phys
(2014) 38: 314 – 322

doi:10.3906/fiz-1405-11

III-Nitride quantum dots in nanowires: growth, structural, and optical properties

Bruno DAUDIN[1,2,*]
[1]University of Grenoble - Alpes, Grenoble, France
[2]Atomic Energy and Alternative Energies Commission (CEA), Institute for Nanoscience and Cryogenics-Physics of Materials and Microstructures (INAC-SP2M), Grenoble, France

Received: 16.05.2014 • **Accepted:** 20.05.2014 • **Published Online:** 10.11.2014 • **Printed:** 28.11.2014

Abstract: Nanowires (NWs) have emerged as a platform to build complex, self-assembled, defect-free nanostructures. In particular, the growth of single islands/disks of various III-nitride combinations (InGaN in GaN, GaN in AlN, AlGaN in AlN) are possible in NW heterostructures, extending the field of experimental quantum dot exploration. Specific to NWs, the possibility to disperse them paves the way to probe and investigate only a single wire/dot.

In the present article, the growth of GaN disks/islands and InGaN islands as well as their optical properties at the nanometer scale will be reviewed. Besides the intentional growth of QD-in NW heterostructures, special attention will be paid to compositional fluctuations in ternary alloy nanowires, which also lead to a quantum dot-like behavior. Specific to NW geometry, optical emission is expected to exhibit a high degree of polarization along the NW axis, opening a pathway to the practical realization of polarized single photon emitters in a wide range of wavelengths.

Key words: Quantum dots-in nanowires, nitrides, GaN, InGaN, AlGaN, quantum confinement, biexciton binding energy

1. Introduction

In spite of being the late-comers in the family of semiconductors prone to forming quantum dots (QDs) [1,2], III-nitride materials exhibit specific features that make them subjects of sustained interest. In particular, the wide band-gap values of nitride materials (about 3.47 eV for GaN and 6 eV for AlN) combined with large band offsets result in a strong exciton confinement and make them of potential interest for single photon emission in the ultraviolet range at room temperature. Indeed, such an emission has been recently demonstrated [3], potentially paving the way for the realization of practical devices.

It is now well established that GaN, InGaN, or AlGaN QDs can be grown by taking advantage of the Stranski–Krastanow (SK) growth mode. In this growth mode, the compressive stress experienced by GaN deposited on AlN or AlGaN, by InGaN deposited on GaN, or by AlGaN deposited on AlN first results in the formation of a strained wetting layer matched to the substrate followed by subsequent elastic relaxation of strain energy by formation of 3D islands above a certain critical thickness. Following the first demonstration of GaN QD growth of Al-polar AlN [1], it was further shown that the SK growth mode was also effective to grow N-polar GaN QDs on N-polar AlN [4], zinc blende GaN QDs [5,6], a-plane [7] and m-plane [8,9] GaN QDs, and semipolar GaN QDs [10]. More recently, as will be extensively discussed later in this review, the growing interest in nitride nanowires (NWs) has provided an alternative solution to the growth of QDs, by taking advantage of

*Correspondence: bruno.daudin@cea.fr

the reduced diameter of NWs and the possibility to grow heterostructures with short sections of a relatively low band-gap material inserted in a NW section of a barrier nitride material.

One of the difficulties to achieve single photon emission using GaN QDs has to do with being able to probe only one single dot, which implies controlling the nucleation process and the QD density. This is not an easy task when considering that nucleation of GaN QDs grown by plasma-assisted molecular beam epitaxy (MBE) on AlN is of extrinsic nature, occurring in the vicinity of threading edge dislocations [11]. Actually, most results published to date refer to AlN templates grown on sapphire or silicon, which exhibit a large density of dislocations, leading to a typical GaN QD density of about $10^{10}/\mathrm{cm}^2$. Such a high density makes the selection of single QDs exceedingly difficult and usually requires a technological step for the fabrication of mesas, each containing a tractable number of QDs. In contrast, QD-in-nanowires are far more easy to isolate, only requiring dispersion of NWs on a suitable substrate for single dot spectroscopy experiments. It is the goal of this article to review the growth process and the structural and optical properties of QDs-in-NWs and to identify the conditions required to achieve single photon emission in a wide range of wavelengths.

2. Growth of QDs-in-NWs

Due to the large aspect ratio (height/diameter) of NWs and the associated large free surface, relatively large critical thicknesses of mismatched heterostructures are expected in the case of NWs with respect to their bidimensional (2D) counterparts. Accordingly, it is theoretically predicted that the formation of fully strained axial and core-shell NW heterostructures should be observed in a wide range of lattice mismatch values [12–14]. Recently, it has been further shown for axial heterostructures that depending on in-plane lattice mismatch and NW diameter, the growth of disks could be favored with respect to the formation of 3D islands [15]. As a matter of fact, an in-plane lattice mismatch of 3%, typically corresponding to the growth of GaN on AlN or of $In_{0.25}Ga_{0.75}N$ on GaN, leads to the formation of QDs obeying the SK growth mode in the case of 2D layer heterostructures [16]. In contrast, for the same combination of materials, it is shown in Figure 1 that NW morphology is expected to result in disk formation for a NW radius smaller than about 20 nm.

2.1. The case of spontaneously nucleated NWs grown by molecular beam epitaxy

Following the pioneering work of Kishino and collaborators [17] and Calleja and collaborators [18] on the growth by MBE of spontaneously nucleated GaN NWs, numerous groups worldwide have investigated the growth conditions of such NWs as a function of substrate nature and growth parameters. As a general feature, such NWs are found to exhibit a reduced diameter, in the range of some tens of nanometers, making them particularly suitable for the growth of heterostructures obeying specific, NW diameter-dependent, strain relaxation mechanisms.

As an experimental evidence of the above statements, Figures 2a–2c show nanodisks (NDs) of GaN embedded in an AlN NW section grown on top of GaN NWs. Whereas growth of GaN on a 2D AlN layer invariably results in the formation of GaN QDs according to the SK growth mode, it appears that NW morphology indeed leads to the growth of GaN NDs. In the case of a large in-plane lattice mismatch insufficiently accommodated by NW geometry, the formation of 3D islands is preferred, as illustrated in Figure 2c by a picture exemplifying the growth of high In content InGaN islands on top of a GaN NW [19,20].

Recent theoretical investigations have established that kinetically driven phase separation may appear in such ternary heterostructures, depending on the particulars of the growth mode, on surface diffusion of different atomic species, and on the lattice mismatch between the substrate and the islands [21]. In accordance with

these predictions, it has been found that individual InGaN dot-in-NWs, such as the ones shown in Figure 2c, indeed exhibit an In content gradient from the base to the top, related to the easy elastic deformation of the tip

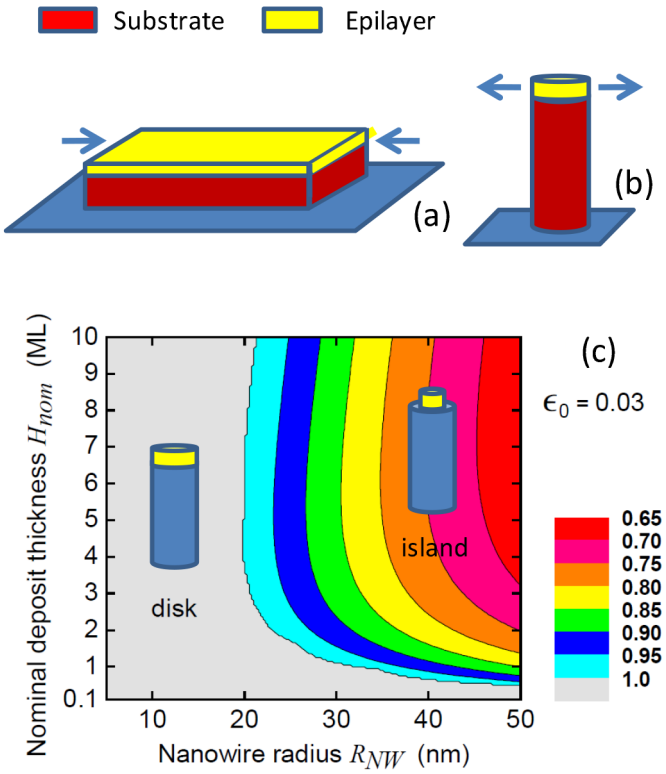

Figure 1. (a) Schematic view of 2D heterostructure growth: the epilayer with a larger in-plane lattice parameter than the substrate is experiencing a biaxial strain. (b) In the case of NW geometry elastic relaxation of the epilayer is made easy. (c) Map of the variations as a function of NW radius and nominal deposit thickness of the ratio W_{opt}/W_{disk} of the minimum energy of the system (at given deposited volume) to its energy in the disk configuration. The nominal deposit thickness is expressed in monolayers of thickness of 0.27 nm. The misfit ε_0 of the deposit with respect to the NW is 3%. The gray zones at left and bottom are where the disk is favored (ratio equal to 1), whereas island formation is preferred in the colored areas. Material parameters: $\nu = 0.33$, E = 3.24×10^{11} Pa, $\gamma_{SW} = 1.8$ J/m^2 (after [15]).

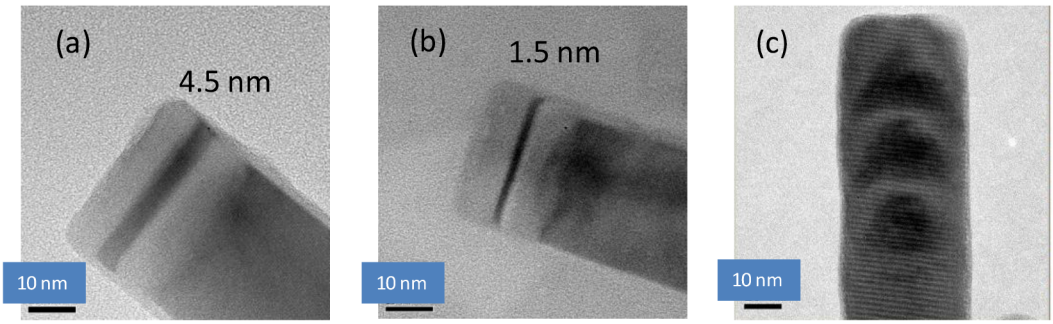

Figure 2. (a) Disk of GaN, 4.5 nm thick, inserted in an AlN NW section grown on top of a GaN NW; (b) 1.5-nm disk; (c) stacking of InGaN islands-in-NW.

of the island. Furthermore, the total In content in each dot has been found to increase from the first to the last, which has been assigned to the progressive elastic strain relaxation of the GaN/InGaN superlattice, making In incorporation progressively easier when going from one island of the stacking to the next above it [19].

Interestingly, the morphological properties of GaN insertion in AlN NWs are very similar to those of standard SK GaN QDs grown on 2D AlN layers by MBE. This statement is illustrated in Figure 3, which compares SK GaN QDs (Figure 3a) with GaN insertions in AlN NWs (Figure 3b). Similar to the case of conventional SK QD stacking, it has been demonstrated that the GaN/AlN superlattices are in elastic equilibrium, with GaN insertions and AlN spacers compressively strained (respectively expanded) by the surrounding material [22]. However, in the case of NWs, it is expected that the GaN dot-in wire strain state is smaller than in the case of stacked SK QDs, a feature specifically assigned to NW geometry and related to the large amount of free surface, which is favorable to elastic strain relaxation [13]. Nevertheless, due to the reduced diffusion length of Al, it is found that capping of GaN insertions by an AlN section systematically results in the formation of a thin AlN shell, which contributes to straining the GaN dot-in wire. The thickness of this AlN shell is found to be proportional to the thickness of the upper AlN section. Depending on the thickness, it has been furthermore established that the AlN shell may be either fully strained or partially plastically relaxed, with concomitant formation of dislocation above a critical shell thickness [23,24]. The formation of an AlN shell due to reduced Al diffusion has also been observed in the case of AlGaN/GaN or AlGaN/AlN NW heterostructures and has been found to affect optical properties of AlGaN/GaN NW superlattices, depending on the thickness of the AlN shell coating [25].

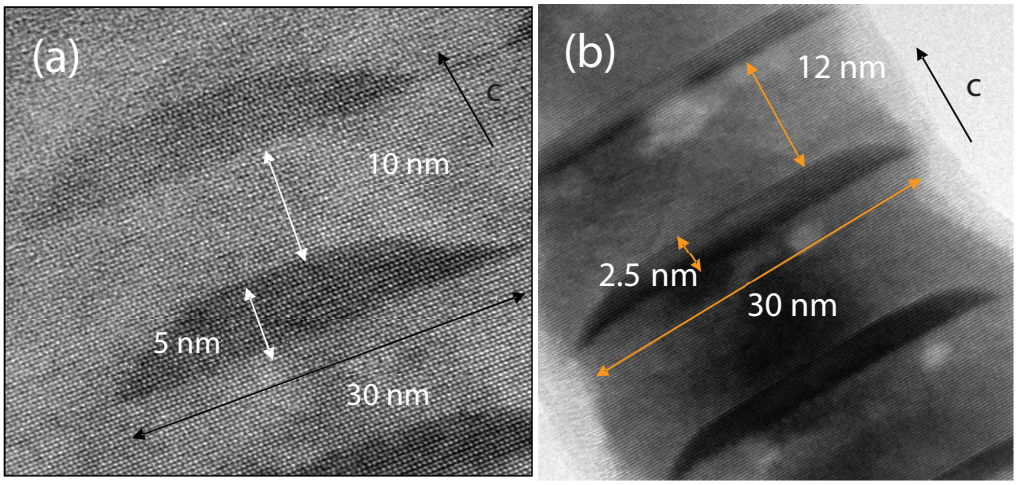

Figure 3. (a) Stack of SK GaN QDs grown by MBE on AlN; (b) stack of GaN insertions in AlN NW section grown by MBE on top of a GaN NW. Note the similarity of dimensions.

2.2. Selective area growth of NWs

An attractive alternative to spontaneously grown NW is selective area growth using patterned substrates, which has been extensively exploited in both MBE and metal organic chemical vapor deposition growth techniques, with the ultimate goal of producing in-plane ordered NWs. The process commences with a Ga-polar GaN layer grown on sapphire, which is subsequently patterned by electron beam lithography to produce windows as small as some hundreds of nanometers. Growth on the aforementioned template results in the formation of position-controlled GaN pyramids. The potential of such pyramids for the growth of arrays of InGaN nanostructures

was identified long ago: indeed, deposition of InGaN on fully formed, untruncated GaN pyramids and further covering with GaN barrier/cap layer leads to the formation of inclined InGaN quantum wells on the side facets [26]. In addition, it has been further demonstrated that this technique also leads to formation of QDs at the apex of the pyramid [27,28].

In recent years, the proper control of substrate (sapphire), nucleation, and growth conditions has allowed one to extend the above technique to the growth of metal-polar GaN NWs, with a faceted top. Further deposition of an InGaN island on top of the faceted GaN NW followed by subsequent GaN capping has led to the formation of single InGaN QDs [29]. Similarly, the growth of a thin AlGaN shell around the GaN core, followed by the deposition of GaN and subsequent capping by AlGaN, has resulted in the formation of single GaN dots at the tip of the NW heterostructures, which were embedded in AlGaN barrier as depicted in the schematic of Figure 4 [30,31].

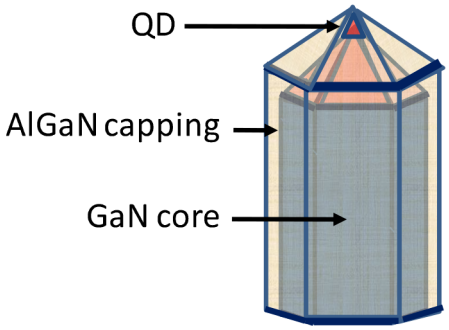

Figure 4. Schematics of QD dot growth on top of NWs obtained by selective area growth on a patterned substrate.

Compared to the standard SK growth mode which relies on a significant lattice mismatch between the dot-forming material and that of the barrier, the use of NWs with faceted tips allows one to grow single QDs, regardless of lattice mismatch. This is particularly interesting in the case of ternary alloys, namely InGaN and AlGaN, virtually extending the possibilities of growing single dots to the whole range of compositions, while making the selection of a single NW for single QD studies relatively easy.

3. Optical properties of QDs-in-NWs

It was discussed above that the morphology of nitride NW heterostructures depends on the lattice mismatch between the dot-forming material and that of the barrier as well as on parameters specific to NW geometry such as the diameter [15]. However, even in the case of 2D growth resulting in the formation of disk-in NWs, the lateral limitation of the active region and the absence of extended defects (excepting the notorious defect consisting of the surface itself) actually lead to a QD behavior. Hence, contrary to the 2D counterpart case, for which free displacement of carriers in the plane makes them sensitive to nonradiative recombination associated with the presence of extended defects, the optical properties of both disk-in NWs and 3D QD-in NWs are expected to be confinement-dominated.

As a consequence of the noncentrosymmetry of wurtzite structure, it is well known that the optical properties of nitride quantum wells and QDs are partially governed by the presence of an internal electric field, consisting of a spontaneous polarization component and a piezoelectric one. The presence of such an electric field has been identified in the case of GaN quantum disks embedded in AlN NW section (see Figure 5a),

leading to a red shift of the photoluminescence (PL) peak for thick nanodisks [32]. However, this red shift is significantly reduced when compared to the case of SK QDs with similar height, a feature which has been theoretically studied by Camacho et al. and has been assigned to the eased elastic strain relaxation specific to NW heterostructures [33].

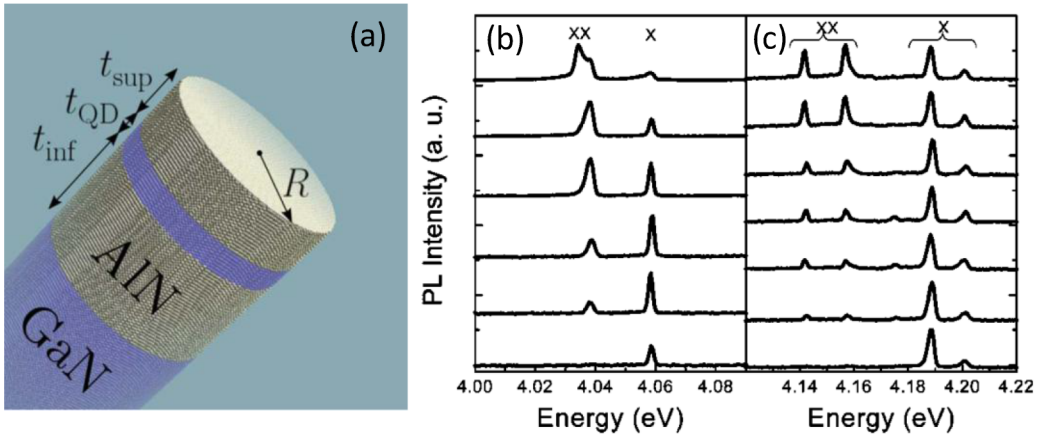

Figure 5. (a) Schematics of GaN QD-in NW samples. (b) Power-dependent spectra of quantum dots' emissions at 5 K. Each spectrum has been normalized to its maximum intensity. Excitation power (increasing from the bottom): 10, 50, 100, 200, 300, and 500 μW. (c) Spectra corresponding to another NW. Excitation power (increasing from the bottom): 25, 100, 120, 170, 200, 250, and 300 μW.

The above mentioned authors [33] also analyzed the electric field experienced by the disk-like GaN QD as a function of the geometrical parameters, shown in Figure 5a. It has been demonstrated that the Fermi level pinning at the upper surface of the NW heterostructure plays a determinant role, making the parameter t_{sup}, in particular, an important component for the precise determination of the electric field experienced by the GaN QD [33].

As mentioned above, the GaN insertions, schematically represented in Figure 5a, are expected to behave as QDs in spite of their 2D morphology, a consequence of their limited diameter associated with an absence of extended defects. Consistent with this statement, autocorrelation experiments performed on GaN disks have revealed the presence of an antibunching dip reaching a value smaller than 0.5, thus demonstrating the single discrete level character of the emitter [32]. Furthermore, PL experiments as a function of laser excitation power have led to identification of excitonic and biexcitonic recombinations stemming from single GaN/AlN quantum dots embedded in nanowires. For such small quantum dots (around 1 nm in height), the low-temperature emission energy is observed above the band gap of GaN between 3.8 and 4.2 eV. The typical full widths at half maximum are in the range between 1 and a few meV, while the biexciton binding energy is between 20 and 40 meV, as illustrated in Figures 5b and 5c [34]. Similar experiments were recently performed by Choi et al. on GaN QDs grown at the tip of a facetted GaN NW, according to the scheme in Figure 4, and led to the determination of a record biexciton binding energy of 52 meV. This is consistent with the general experimental observation of increasing binding energy values for increasing emission energies, as shown in Figure 6, along with results extracted from optical experiments performed on standard SK GaN QDs [35–37].

Turning now our attention to the ternary alloys, PL experiments on InGaN disks inserted in GaN NWs have also been performed [38], confirming the QD-character of such nanodisks as an illustration of the possibility

to easily isolate a single NW. This, combined with the absence of background emission, makes QDs-in NW ideal systems for single QD spectroscopic studies. This potential was exploited by Deshpandhe et al., who grew InGaN/GaN NW heterostructures and demonstrated single photon emitter properties of InGaN QD-in NWs [39].

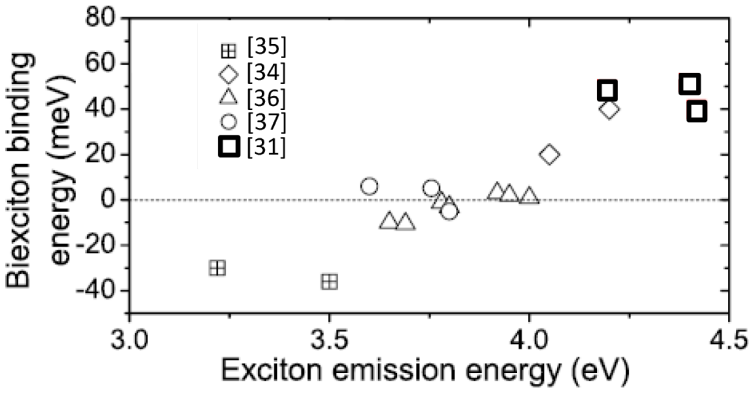

Figure 6. Biexciton binding energy of GaN QDs as a function of exciton emission energy. Results of [31] and [34] refer to QDs in NWs (after [31]).

While all works mentioned above concern the intentional growth of QD-in NW, it has to be stressed that InGaN and AlGaN NWs exhibit peculiar optical properties, consistent with the presence of localization centers behaving as unintentionally grown QDs-in NWs. As a matter of fact, reduced thermal quenching of PL intensity has been observed in the case of InGaN [40] and AlGaN [41,42] NWs, as a clue of carrier localization. In the particular case of AlGaN NWs, micro-PL experiments on single NWs have demonstrated the presence of a reduced number of very sharp lines consistent with the presence of carrier localization centers behaving as QDs-in NWs, opening the way to the detailed optical study of nanometric amounts of AlGaN alloys [42].

Besides the possibility of being able to easily separate the NWs from their substrate, which makes available tiny amounts of material for studying structural and optical properties at the nanometric scale, the geometry itself of NWs leads to peculiar effects. As a matter of fact, it is expected that the large dielectric index contrast between the NWs and the surrounding medium, combined with the elongated geometry of the NWs, will favor absorption and emission of light polarized along the growth axis compared to light with electric field perpendicular to the growth axis. Such a behavior was experimentally observed by Rigutti et al. [43]. In addition, those authors studied the optical properties of $Al_xGa_{1-x}N$/GaN multiquantum-disks and found that the 2 main luminescence contributions are mutually perpendicularly polarized, a behavior assigned to the peculiar geometry of these NW heterostructures [43].

These results open the way for potential application of QD-in NWs heterostructures for polarized light emitters/detectors, with no need of an external polarizer. As an example of such applications, it was recently shown that nano-LED emitting in the visible range could be achieved. They consisted of single NW heterostructures with an InGaN disk as the active region [43–45]. Single photon emission with a high degree of linear polarization along the c axis of the nanowire has been observed, as a further illustration of the potential of QD-in NW heterostructures for the realization of polarized single photon emitters in a wide wavelength range, from infrared and visible to ultraviolet.

4. Conclusions

The data presented indicate that QD-in NWs open a new path for the study of single QDs. Contrary to the standard approach, which often requires a technological step to define mesas in a bidimensional layer containing a large number of QDs grown by the Stranski–Krastanow growth mode, the facile separation of NWs from their substrate indeed makes it relatively easy to probe single objects containing one or a limited number of QDs. In the case of the nitride materials that have been examined here, the NW geometry and the easy strain relaxation resulting from a large amount of free surface in NWs also contributes to the reduction of the internal electrical field responsible for the quantum-confined Stark effect and increase of the recombination efficiency in NW heterostructures with respect to their bidimensional counterparts. Although the study of structural and optical properties of ternary alloys is generally limited to the size of the probe, single InGaN and AlGaN NWs provide easy access to tiny amounts of ternary alloys, making possible their study at the nanometer scale. Such a study has already revealed that composition fluctuations in ternary alloy NWs exhibit a quantum dot-like behavior. Finally, the high degree of polarization of the emitted light along the NW axis, intrinsically resulting from NW geometry, also brands NWs as a new class of objects, paving the way to the practical realization of polarized single photon emitters in a wide range of wavelengths.

References

[1] Daudin, B.; Widmann, F.; Feuillet, G.; Samson, Y.; Arlery, M.; Rouvière, J. L. *Phys. Rev. B* **1997**, *56*, R7069–R7072.

[2] Widmann, F.; Daudin, B.; Feuillet, G.; Samson, Y.; Rouvière, J. L.; Pelekanos, N. *J. Appl. Phys.* **1998**, *83*, 7618–7624.

[3] Holmes, M. J.; Choi, K.; Kako, S.; Arita, M.; Arakawa, Y. *Nano Lett.* **2014**, *14*, 982–986.

[4] Gogneau, N.; Sarigiannidou, E.; Monroy, E.; Monnoye, S.; Mank, H.; Daudin, *B. Appl. Phys. Lett.* **2004**, *85*, 1421–1423.

[5] Martinez-Guerrero, E.; Adelmann, C.; Chabuel, F.; Simon, J.; Pelekanos, N. T.; Mula, G.; Daudin, B.; Feuillet, G.; Mariette, H. *Appl. Phys. Lett.* **2000**, *77*, 809–811.

[6] Martinez-Guerrero, E.; Bellet-Amalric, E.; Martinet, L.; Feuillet, G.; Daudin, B.; Mariette, H.; Holliger, P.; Dubois, C.; Bru-Chevallier, C.; Aboughe Nze, P. et al. *J. Appl. Phys.* **2002**, *91*, 4983–4987.

[7] Founta, S.; Rol, F.; Bellet-Amalric, E.; Bleuse, J.; Daudin, B.; Gayral, B.; Mariette, H.; Moisson, C. *Appl. Phys. Lett.* **2005**, *86*, 171901–171903.

[8] Amstatt, B.; Renard, J.; Bougerol, C.; Bellet-Amalric, E.; Gayral B.; Daudin, B. *J. Appl. Phys.* **2007**, *102*, 074913–074920.

[9] Amstatt, B.; Landré, O.; Favre Nicolin, V.; Proietti, M. G.; Bellet-Amalric, E.; Bougerol, C.; Renevier, H.; Daudin, B. *J. Appl. Phys.* **2008**, *104*, 063521–063526.

[10] Lahourcade, L.; Valdueza-Felip, S.; Kehagias, T.; Dimitrakopulos, G. P.; Komninou, P.; Monroy, E. *Appl. Phys. Lett.* **2009**, *94*, 111901–111903.

[11] Rouvière, J. L.; Simon, J.; Pelekanos, N.; Daudin, B.; Feuillet, G. *Appl. Phys. Lett.* **1999**, *75*, 2632–2634.

[12] Ertekin, E.; Greaney, P. A.; Chrzan, D. C. *J. Appl. Phys.* **2005**, *97*, 114325–114334.

[13] Glas, F. *Phys. Rev. B* **2006**, *74*, 121302(R)–121305(R).

[14] Raychaudhuri, S.; Yu, E. T. *J. Appl. Phys.* **2006**, *99*, 114308–114314.

[15] Glas, F.; Daudin, B. *Phys. Rev. B* **2012**, *86*, 174112–174119.

[16] Adelmann, C.; Simon, J.; Feuillet, G.; Pelekanos, N. T.; Daudin, B.; Fishman, G. *Appl. Phys. Lett.* **2000**, *76*, 1570–1572.

[17] Yoshizawa, M.; Kikuchi, A.; Mori, M.; Fujita, N.; Kishino, K. *Jpn. J. Appl. Phys.* **1997**, *36*, L459–L462.

[18] Sanchez-Garcia, M. A.; Calleja, E.; Monroy, E.; Sanchez, F. J.; Calle, F.; Muñoz, E.; Beresford, R. *J. Cryst. Growth* **1998**, *183*, 23–30.

[19] Tourbot, G.; Bougerol, C.; Glas, F.; Zagonel, L. F.; Mahfoud, Z.; Meuret, S.; Gilet, P.; Kociak, M.; Gayral B.; Daudin, B. *Nanotechnology* **2012**, *23*, 135703–135708.

[20] Chang, Y. L.; Wang, J. L.; Li, F.; Mi, Z. *Appl. Phys. Lett.* **2010**, *96*, 013106–013108.

[21] Niu, X.; Stringfellow, G. B.; Liu F. *Appl. Phys. Lett.* **2011**, *99*, 213102–213104.

[22]] Landré, O.; Camacho, D; Bougerol, C.; Niquet, Y. M.; Favre-Nicolin, V.; Renaud, G.; Renevier, H.; Daudin, B. *Phys. Rev. B* **2010**, *81*, 153306–153309.

[23] Bougerol, C.; Songmuang, R.; Camacho, D.; Niquet, Y. M.; Mata, R.; Cros, A.; Daudin, B. *Nanotechnology* **2009**, *20*, 295706–295710.

[24] Hestroffer, K.; Mata, R.; Camacho, D.; Leclere, C.; Tourbot, G.; Niquet, Y. M.; Cros, A.; Bougerol, C.; Renevier, H.; Daudin, B. *Nanotechnology* **2010**, *21*, 415702–415708.

[25] Zagonel, L. F.; Mazzucco, S.; Tencé, M., March, K.; Bernard, R.; Laslier, B.; Jacopin, G.; Tchernycheva, M.; Rigutti, L.; Julien, F. H. et al. *Nano Lett.* **2011**, *11*, 568–573.

[26] Kapolnek, D.; Keller, S.; Underwood, R. D.; DenBaars, S. P.; Mishra, U. K. *J. Cryst. Growth* **1998**, *189/190*, 83–86.

[27] Tachibana, K.; Someya, T.; Ishida, S.; Arakawa, Y. *Appl. Phys. Lett.* **2000**, *76*, 3212–3214.

[28] Lundskog, A.; Palisaitis, J.; Hsu, C. W.; Eriksson, M.; Karlsson, K. F.; Hultman, L.; Persson, P. O. A.; Forsberg, U.; Holtz, P. O.; Janzen, E. *Nanotechnology* **2012**, *23*, 305708–305713.

[29] Kim, J. H.; Ko, Y. H.; Gong, S. H.; Ko, S. M.; Cho, Y. H. *Sci. Rep.* **2013**, *3*, 2150–2156.

[30] Choi, K.; Arita, M.; Arakawa, Y. *J. Cryst. Growth* **2012**, *357*, 58–61.

[31] Choi, A. K.; Kako, S.; Holmes, M. J; Arita, M.; Arakawa, Y. *Appl. Phys. Lett.* **2013**, *103*, 171907–171910.

[32] Renard, J.; Songmuang, R.; Tourbot, G.; Bougerol, C.; Daudin B.; Gayral, B. *Phys. Rev. B* **2009**, *80*, 121305–121308.

[33] Camacho, D.; Niquet, Y. M. *Phys. Rev. B* **2010**, *81*, 195313–195322.

[34] Renard, J.; Songmuang, R.; Bougerol, C.; Daudin, B.; Gayral, B. *Nano Lett.* **2008**, *8*, 2092–2096.

[35] Miyamura, M.; Tachibana, K.; Arakawa, Y. *Appl. Phys. Lett.* **2002**, *80*, 3937–3939.

[36] Simeonov, D.; Dussaigne, A.; Butté, R.; Grandjean, N. *Phys. Rev. B* **2008**, *77*, 075306–075310.

[37] Amloy, S.; Yu, K. H.; Karlsson, K. F.; Farivar, R.; Andersson,T. G.; Holtz, P. O. *Appl. Phys. Lett.* **2011**, *99*, 251903–251905.

[38] Bardoux, R.; Kaneta, A.; Funato, M.; Kawakami, Y.; Kikuchi, A.; Kishino, K. *Phys. Rev. B* **2009**, *79*, 155307–155312.

[39] Deshpande, S.; Das, A.; Bhattacharya, P. *Appl. Phys. Lett.* **2013**, *102*, 161114–161118.

[40] Tourbot, G.; Bougerol, C.; Grenier, A.; Den Hertog, M.; Sam-Giao, D.; Cooper, D.; Gilet, P.; Gayral, B.; Daudin, B. *Nanotechnology* **2011**, *22*, 075601–075608.

[41] Pierret, A.; Bougerol, C.; Gayral, B.; Kociak, M.; Daudin, B.*Nanotechnology* **2013**, *24*, 305703–305709.

[42] Pierret, A.; Bougerol, C.; Den Hertog, M.; Gayral, B.; Kociak, M.; Renevier, H.; Daudin, B. *Phys. Stat. Sol. (RRL)* **2013**, *7*, 868–873.

[43] Rigutti, L.; Tchernycheva, M.; De Luna Bugallo, A.; Jacopin, G.; Julien, F. H.; Furtmayr, F.; Stutzmann, M.; Eickhoff, M.; Songmuang, R.; Fortuna, F. *Phys. Rev. B* **2010**, *81*, 045411–045419.

[44] Deshpande, S.; Bhattacharya, P. *Appl. Phys. Lett.* **2013**, *103*, 241117–241121.

[45] Deshpande, S.; Heo, J.; Das, A.; Bhattacharya, P. *Nature Communications* **2013**, *4*, 1675–1682.